# Superconductivity in multiple phases of compressed $GeSb_2Te_4$

E. Greenberg,[1] B. Hen,[1] Samar Layek,[1] I. Pozin,[2] R. Friedman,[3] V. Shelukhin,[1] Y. Rosenberg,[4] M. Karpovski,[1] M. P. Pasternak,[1] E. Sterer,[3] Y. Dagan,[1] G. Kh. Rozenberg,[1] and A. Palevski[1,*]

[1]*Raymond and Beverly Sackler School of Physics and Astronomy, Tel Aviv University, Tel Aviv 69978, Israel*

[2]*Department of Material Science and Engineering, Tel Aviv University, Tel Aviv 69978, Israel*

[3]*Physics Department, Nuclear Research Center Negev, P.O. Box 9001, Beer Sheva 84190, Israel*

[4]*Wolfson Applied Material Research Center, Tel Aviv University, Tel Aviv 69978, Israel*

(Received 9 May 2016; revised manuscript received 25 January 2017; published 23 February 2017)

Here we report the discovery of superconductivity in multiple phases of the compressed $GeSb_2Te_4$ (GST) phase change memory alloy, which has attracted considerable attention for the last decade due to its unusual physical properties with many potential applications. Superconductivity is observed through electrical transport measurements, both for the amorphous ($a$-GST) and for the crystalline ($c$-GST) phases. The superconducting critical temperature $T_c$ continuously increases with applied pressure, reaching a maximum $T_c = 6$ K at $P = 20$ GPa for $a$-GST, whereas the critical temperature of the cubic phase reaches a maximum $T_c = 8$ K at 30 GPa. This material system, exhibiting a superconductor-insulator quantum phase transition, has an advantage over disordered metals since it has a continuous control of the crystal structure and the electronic properties using pressure as an external stimulus.

DOI: 10.1103/PhysRevB.95.064514

## I. INTRODUCTION

In conventional metals and alloys Coulomb interactions are screened by the conducting electrons, but an attraction between electrons due to the electron-phonon interaction results in superconductivity, which appears at a critical temperature $T_c$ determined by the Debye frequency and the electron-phonon coupling constant. A system where the electronic properties can be tuned and the material can undergo a transition from a metallic to an insulating state by applying an external stimulus can therefore become a laboratory for studying fundamental questions about superconductivity and quantum phase transitions.

$GeSb_2Te_4$ (GST) is a phase change material whose unusual physical properties [1–6] promise many potential applications in the electronics industry [7–10]. GST can undergo a reversible change from an amorphous phase ($a$-GST) to a crystalline ($c$-GST) one at elevated temperatures [1–4], but also by elevated pressure at ambient temperature [11]. This transition is accompanied by a significant change of over four decades in resistance. The observed resistance changes, as well as a reversible $a$-GST to $c$-GST phase transition, have been explained using numerical simulations [11–13]. The corresponding metal-to-insulator transition (MIT) in GST is often explained as a disorder-induced Anderson localization [1].

Superconductivity near a metal-to-insulator transition has been reported in disordered metals [14] and has been studied intensively. Nevertheless, a continuous control of the electronic properties using external stimuli has been lacking. Here, using pressure as an external stimulus, we show that GST becomes superconducting at low temperature and elevated pressure, while preserving its structural symmetry, namely, remaining in the amorphous state. Therefore, amorphous GST becomes an excellent tunable system for studying three-dimensional superconductor-insulator quantum phase transitions. Furthermore, we demonstrate that superconductivity with a somewhat higher $T_c$ is observed at higher pressures when the material undergoes a structural transition from the amorphous ($a$-GST) into the crystalline ($c$-GST) phase.

## II. RESULTS AND DISCUSSIONS

In our transport studies of GST material under pressure in a wide temperature range, we used as-grown amorphous ($a$-GST) and as-prepared crystalline ($c$-GST) powders; pressure was generated using diamond anvil cells (DACs); electrical transport measurements were performed using a physical property measurement system (for details, see the Supplemental Material (SM) [15]). The lattice of $c$-GST is hexagonal at ambient temperature and atmospheric pressure, and therefore the crystalline samples are denoted as $h$-GST in their initial conditions. An x-ray diffraction analysis of our amorphous and crystalline samples, shown in SM [15] (Fig. S1), confirms the amorphous structure of as-prepared $a$-GST and the hexagonal structure of $h$-GST. Upon application of pressure at ambient temperature we observe (SM [15], Fig. S2), in agreement with Ref. [16], a gradual change in the density of the amorphous GST material, which becomes almost constant for pressures above 14 GPa, followed by crystallization into a bcc lattice at pressures above 20 GPa.

We emphasize that the continuous densification observed in the amorphous phase should not be confused with the structural phase transition with a symmetry change such as the one observed at crystallization into a bcc lattice. The structure of GST at a pressure of 10 GPa, where we observe superconductivity, is identical to the one at somewhat below 10 GPa, namely, preserving the same amorphous phase with a somewhat higher density. In fact, the borderline between the low- and high-density amorphous phases is quite arbitrary. The authors of Ref. [16] have used the highest change in densification rate as a criterion for putting the borderline between them. For our sample, if we use this criterion, the

*apalev@post.tau.ac.il

 

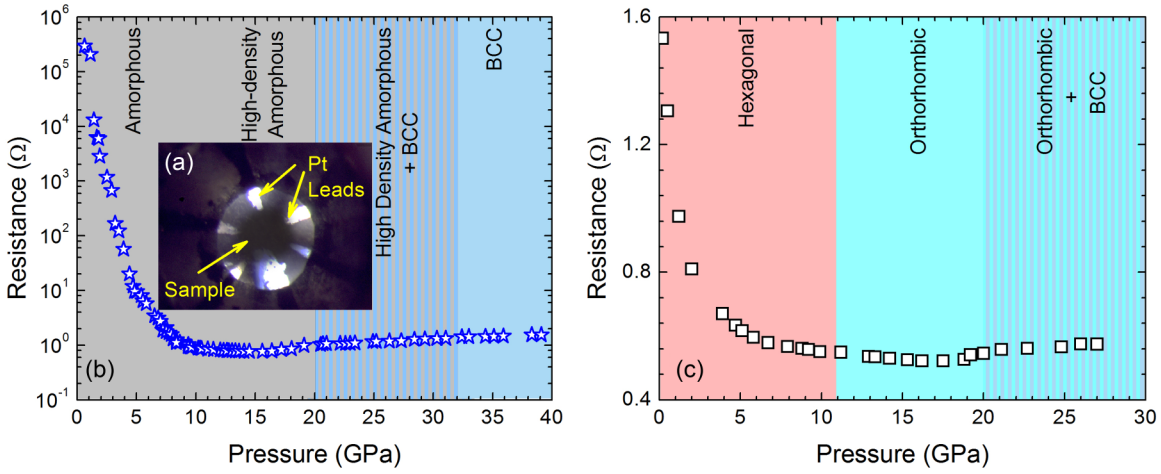


FIG. 1. Room temperature resistance under pressure. (a) Six platinum triangles under pressure in one of the measurement setups. (b) Resistance as a function of pressure of $a$-GST. (c) Pressure dependence of resistance of $c$-GST. Shaded regions in different colors [(in both (b) and (c)] are according to previously published XRD data [16,17] and our resistance measurements.

borderline would be at ∼14 GPa. We also observe all phases of crystallographic transitions reported in Ref. [17] for the initially crystalline $h$-GST (see SM [15], Fig. S2).

Two cells of $a$-GST were prepared (samples 1 and 2), one of which was made of nonmagnetic materials to enable low temperature transport measurements at various magnetic fields (sample 1). Two cells of the $h$-GST sample were also measured as a function of temperature for various pressures. In Fig. 1(a), we show the typical contact configuration for measuring resistance at various pressures as a function of temperature.

At ambient temperature, the $a$-GST samples show a dramatic, over five orders of magnitude, drop in resistance, when it is compressed by applying quasihydrostatic pressure, followed by saturation above 9 GPa, as shown in Fig. 1(b). The behavior of $h$-GST also saturates above 10 GPa, as seen Fig. 1(c), however, the overall change in resistance is much smaller. The dramatic drop in resistance for the $a$-GST sample is corroborated with the corresponding change of the mechanism of conductivity.

For low pressures, below 5 GPa, the variation of resistance versus temperature indicates that the $a$-GST is an Anderson insulator with a typical transition from a simply activated to Mott variable range hopping mechanism of the electronic transport, as depicted in Fig. 2. At pressures exceeding 9.5 GPa, when the resistivity drops below approximately 1 mΩ cm, the value reported previously [1] as a precursor of the metal-insulator transition (MIT), $a$-GST becomes a superconductor (Fig. 2).

In Fig. 3, we show resistance versus temperature for two amorphous samples. The plots in Fig. 3 show that for pressures below $P = 21$ GPa, there is a monotonous increase of the superconductor transition temperature with pressure, accompanied with a decrease of the normal state resistance. The behavior changes drastically when the pressure is further increased above 21 GPa. One can clearly see that the curves have two distinct transitions, signifying the appearance of an additional phase with a higher transition temperature. This double transition is observed in both samples.

As demonstrated by our x-ray diffraction (XRD) data in SM [15], and as was reported previously by others [16], at this range of pressure, a crystallographic phase transition occurs, forming the bcc ordered phase, bcc-GST. We can therefore interpret the double transition as the coexistence of $a$-GST with bcc-GST, both being superconductors with a higher value of $T_c$ for the crystalline phase. In Fig. 4(a), we show magnetoresistance measurements at 2 K for sample 1 at different pressures. From these curves we can extract the upper critical field $H_{C2}$, defined as the field for which the resistance attains half of the normal state resistance value. A closer inspection of the curves shown in Fig. 4(b) reveals a double transition versus magnetic field. These double transitions in the magnetic field appear at a somewhat higher pressure than the corresponding double transitions observed

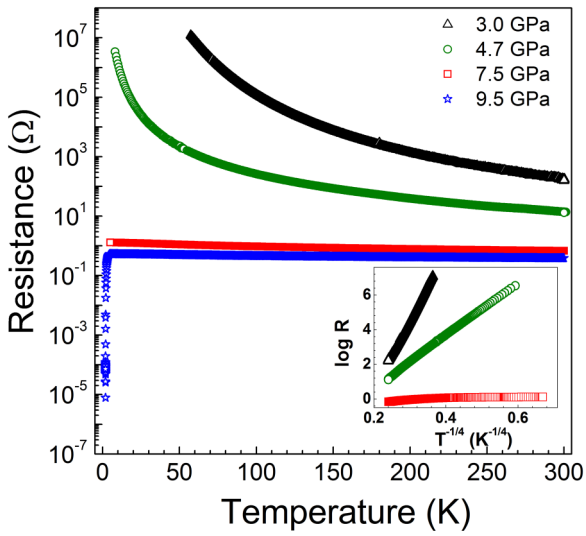


FIG. 2. Temperature dependence of $a$-GST samples demonstrating the superconductor-insulator transition (SIT). The Mott variable range hopping is clearly observed at pressures between 3.0 and 7.5 GPa, as seen from the inset.

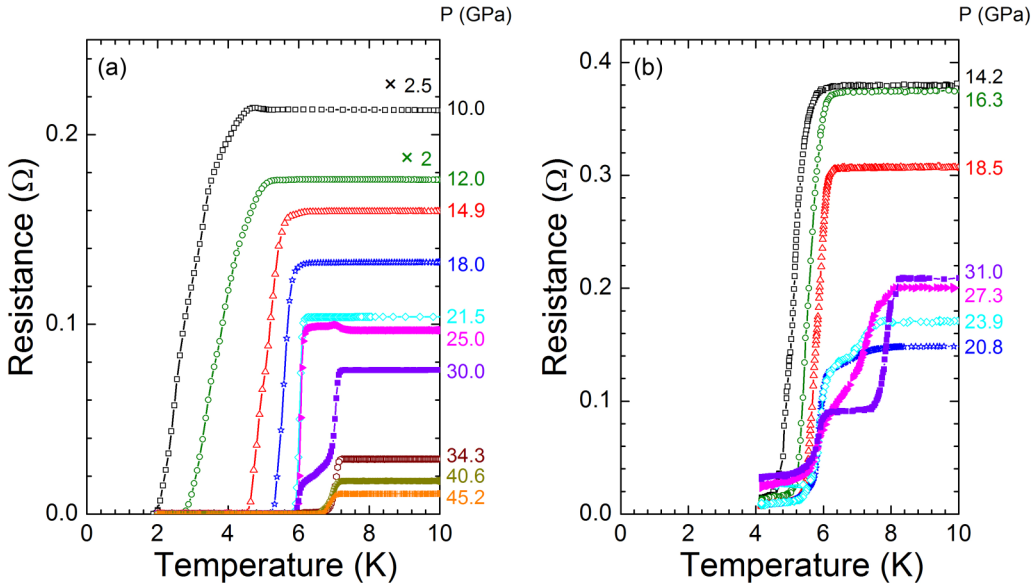


FIG. 3. Superconducting transitions of $a$-GST. (a) Temperature dependence of resistance at different pressures using four-probe geometry (sample 1) and (b) using quasi-four-probe geometry (sample 2). Two distinct superconducting transitions are observed.

in $R(T)$ curves. For these pressures, exceeding 40 GPa, only a single bcc phase is expected to remain. This inconsistency is the subject for further investigation. The values of the corresponding upper critical field are plotted in Fig. 4(c). Our definition of $H_{C2}$ is not appropriate for the pressure range where we observe a double transition (coexistence regime). In the latter case we estimated $H_{C2}$ as the midpoint value of each transition for each phase. Using a typical value of $H_{C2} = 2.8$ T within the Ginzburg-Landau and BCS formalism [18], we estimate the microscopic parameters as follows: the Ginzburg Landau coherence length, $\xi_{GL}(T) \approx 30$ nm at $T \approx 2$ K. Assuming that our samples are in a clean limit, $\ell \geqslant \xi_0$, which is a reasonable assumption for a metallic GST with resistivity $\rho \leqslant 10\ \mu\Omega$ cm, we can estimate the Pippard coherence length at low temperatures to be $\xi_0 \approx 40$ nm. If we assume that the superconducting gap follows BCS theory, $\Delta = 3.5 k_B T_c$, then we can estimate the Fermi velocity by using the relation $\xi_0 = \frac{\hbar v_f}{\pi \Delta}$, and taking $T_c = 7$ K for bcc-GST, we find $v_f \approx 3 \times 10^5$ m/s. Additional current-voltage measurements can be found in SM [15] (Fig. S3).

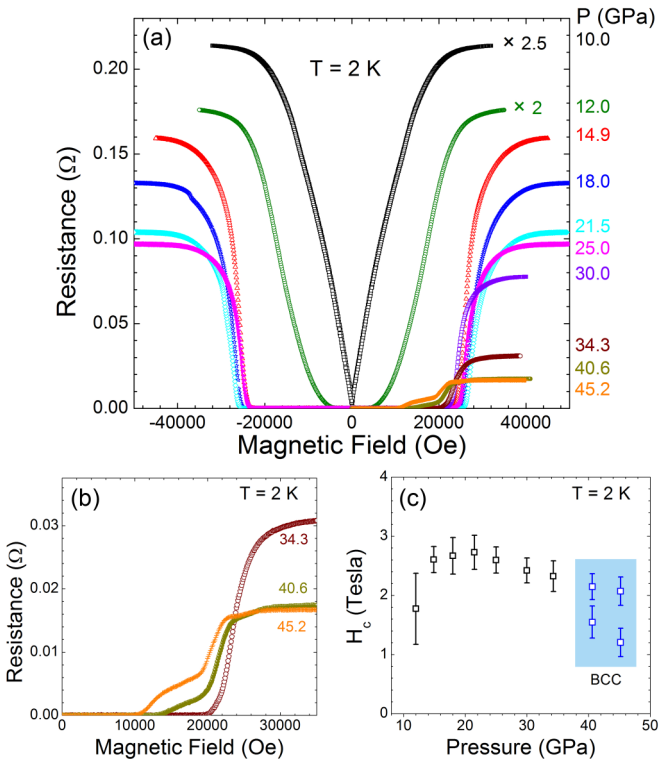


FIG. 4. Pressure dependence of the critical field of $a$-GST (sample 1). (a) Resistance as a function of magnetic field at different pressures. (b) Zoomed portion of the transitions from (a) for 34.3, 40.6, and 45.2 GPa showing two transitions in the last two pressures. (c) Variation of the critical field as a function of pressure.

We also performed low temperature studies on two samples prepared in the hexagonal phase, which were measured in different DACs. As we already mentioned, the behavior of $h$-GST under pressure is quite different: First, the resistivity changes by less than an order of magnitude at 300 K when compressed [see Fig. 1(b)], and second, it exhibits normal metallic behavior at pressures below 10 GPa. The first crystalline sample was compressed at room temperature to 28 GPa, decompressed, and recompressed again. The variation of room temperature resistance upon this cycle is depicted in SM [15] (Fig. S4). Since our as-prepared $a$-GST was superconducting when transformed into the bcc phase, one could expect that the as-prepared $h$-GST sample will also exhibit superconductivity upon compression, following decompression from 28 GPa, where bcc-GST is formed according to SM [15] (Fig. S2) and Ref. [17]. We indeed observe the appearance of superconductivity upon recompression at pressures above 14 GPa, as shown in Fig. 5(b). There are two separate transitions in the $R(T)$ curve which are quite distinct. We attribute the highest $T_c$ to the bcc phase, since it is very close to the value of $T_c$ observed in as-prepared $a$-GST samples undergoing a crystallographic

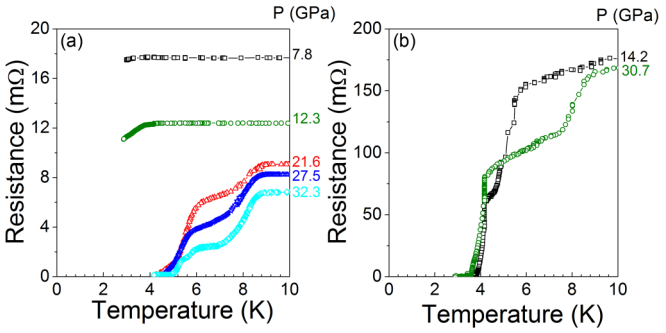


FIG. 5. Superconducting transitions of *c*-GST. (a) Temperature dependence of resistance at different pressures. (b) Same measurements using two wires after subtracting residual resistance values (1.329 and 1.564 Ω for 14.2 and 30.7 GPa, respectively).

transition to the bcc phase, whereas the lower transition is attributed to superconductivity in the orthorhombic phase (see SM [15], Fig. S2, and Ref. [17]). The measurements of the second *h*-GST sample were performed only in the compression mode. These measurements reveal behavior that is similar to the first sample, i.e., they do not exhibit superconductivity at temperatures around 4 K for pressures below 14 GPa [Fig. 5(a)]. At higher pressures, where *h*-GST transforms into different crystallographic phases (SM [15], Fig. S2), we observe superconductivity at the same temperatures as the first sample upon recompression [see Fig. 5(b)]. We use a similar definition for the critical temperature $T_c$ as we used for defining $H_{C2}$, namely, as the temperature for which the value of the resistance is one half of its value at the normal state, prior to the transition. We can get a $T$-$P$ phase diagram, which summarizes our findings for both as-prepared *a*-GST and *h*-GST samples, by plotting the variation of $T_c$ vs $P$ in Fig. 6 for both measurement sets. At the range presented in our phase diagram it appears that the low-density amorphous and the hexagonal phases are not exhibiting superconductivity. Much lower temperatures than those available in our current experimental setup are needed to complete the phase diagram.

## III. CONCLUSIONS

In conclusion, we have demonstrated superconductivity in both amorphous and a few crystalline phases of $GeSb_2Te_4$ compound with a maximum transition temperature of $T_c = 8$ K at a pressure of 30 GPa. We believe that in addition to being a phase change material, GST becomes a laboratory for studying superconductor-to-insulator transitions (SITs) with the pressure being an external tuning parameter. It also provides a unique opportunity to study and compare the disorder-driven SIT quantum phase transition observed in the amorphous phase.

One of the remaining open questions regarding the nature of the observed quantum phase transition [19] in the amorphous phase, which we hope to answer in the future, is the existence of a quantum critical point where $T_c$ vanishes (an Anderson-like transition) or $T_c$ remains finite, indicating a Mott-like transition. Moreover, most of the systems where the SITs were observed are either two dimensional (thin films of InOx, Bi, MoGe, TaN), or almost two dimensional (layered high temperature perovskite superconductors). There are some experimental indications as well as theoretical predictions [20] that there might be an anomalous metallic phase with the high values of conductivity in between the insulating and the superconducting states. The conductivity of this anomalous metal exceeds by orders of magnitude the Drude conductivity in the normal state. Our amorphous GST, being a three-dimensional system, could provide an answer in future studies whether the anomalous metallic phase is not restricted only for two dimensions.

## ACKNOWLEDGMENTS

A.P. would like to acknowledge very helpful discussions with Aharon Kapitulnik, Gabriel Aeppli, Steve Kivelson, Srinivas Raghu, Boris Spivak, and Moshe Goldstein. The authors would like to thank M. Shulman for his help with the

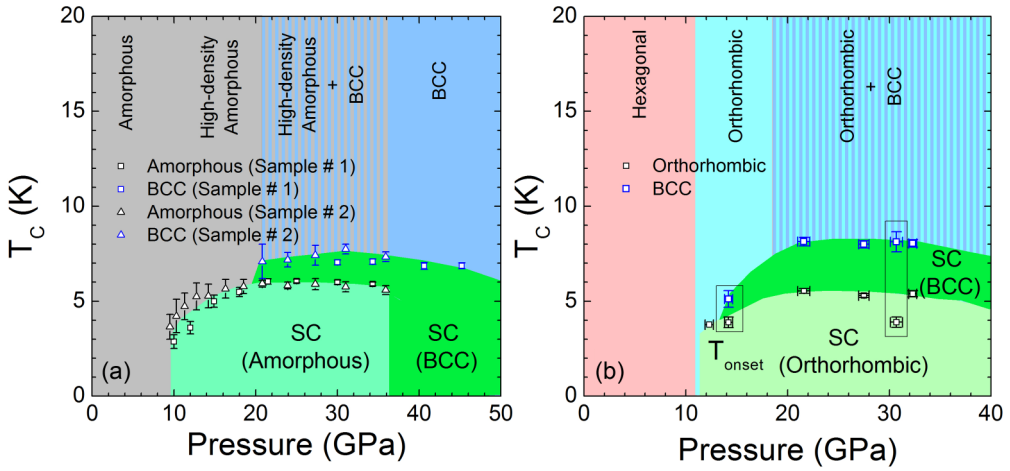


FIG. 6. Superconducting phase diagram of (a) *a*-GST and (b) *c*-GST. Shaded regions in different colors are according to our superconductivity measurements. Since the superconducting transition is not completed at 12.3 GPa, which is the first point in (b), only the onset temperature is given. The points inside rectangles in (b) are measured during the recompression cycle.

variable temperature inset (VTI) system and A. Rabinowicz, A. Ron, and E. Maniv for their assistance. We are grateful to Volodymyr Svitlyk and Andrew Cairns at the ESRF for providing assistance in using beamline ID27. This research was partially funded by the PAZI Foundation under Grant No. 268/15. Support from the Israeli Science Foundation under Grants No. 569/13 and No. 1189/14, and from the Israel Ministry of Science, Technology and Space, under Contract No. 3-11875, are acknowledged.

E.G., B.H., and S.L. contributed equally to this work.

[1] T. Siegrist, P. Jost, H. Volker, M. Woda, P. Merkelbach, C. Schlockermann, and M. Wuttig, Nat. Mater. **10**, 202 (2011).

[2] W. Zhang, A. Thiess, P. Zalden, R. Zeller, P. H. Dederichs, J.-Y. Raty, M. Wuttig, S. Blügel, and R. Mazzarello, Nat. Mater. **11**, 952 (2012).

[3] P. Nukala, R. Agarwal, X. Qian, M. H. Jang, S. Dhara, K. Kumar, A. T. C. Johnson, J. Li, and R. Agarwal, Nano Lett. **14**, 2201 (2014).

[4] K. S. Siegert, F. R. L. Lange, E. R. Sittner, H. Volker, C. Schlockermann, T. Siegrist, and M. Wuttig, Rep. Prog. Phys. **78**, 013001 (2015).

[5] N. P. Breznay, H. Volker, A. Palevski, R. Mazzarello, A. Kapitulnik, and M. Wuttig, Phys. Rev. B **86**, 205302 (2012).

[6] P. Zalden, K. S. Siegert, S. Rols, H. E. Fischer, F. Schlich, T. Hu, and M. Wuttig, Chem. Mater. **26**, 2307 (2014).

[7] D. Loke, T. H. Lee, W. J. Wang, L. P. Shi, R. Zhao, Y. C. Yeo, T. C. Chong, and S. R. Elliott, Science **336**, 1566 (2012).

[8] D. Lencer, M. Salinga, B. Grabowski, T. Hickel, J. Neugebauer, and M. Wuttig, Nat. Mater. **7**, 972 (2008).

[9] M. Wuttig and N. Yamada, Nat. Mater. **6**, 824 (2007).

[10] J. Hegedüs and S. R. Elliott, Nat. Mater. **7**, 399 (2008).

[11] M. Xu, Y. Q. Cheng, L. Wang, H. W. Sheng, Y. Meng, W. G. Yang, X. D. Han, and E. Ma, Proc. Natl. Acad. Sci. U.S.A. **109**, E1055 (2012).

[12] Z. Sun, J. Zhou, Y. Pan, Z. Song, H.-K. Mao, and R. Ahuja, Proc. Natl. Acad. Sci. U.S.A. **108**, 10410 (2011).

[13] M. Xu, W. Zhang, R. Mazzarello, and M. Wuttig, Adv. Sci. **2**, 1500117 (2015).

[14] A. M. Goldman, Int. J. Mod. Phys. B **24**, 4081 (2010).

[15] See Supplemental Material at http://link.aps.org/supplemental/10.1103/PhysRevB.95.064514 for methods and further plots of selected XRD spectra, and plots of critical current and resistance.

[16] B. Kalkan, S. Sen, J.-Y. Cho, Y.-C. Joo, and S. M. Clark, Appl. Phys. Lett. **101**, 151906 (2012).

[17] B. Kalkan, S. Sen, and S. M. Clark, J. Chem. Phys. **135**, 124510 (2011).

[18] M. Tinkham, *Introduction to Superconductivity* (Kreiger, Malabar, FL,1980).

[19] V. F. Gantmakher and V. T. Dolgopolov, Phys. Usp. **53**, 1 (2010).

[20] B. Spivak and S. Kivelson (private communication).